Structure of Hyperlithiated Li_3O and Evidence for Electronomers

Keiichi Yokoyama*

Department of Materials Science, Japan Atomic Energy Research Institute, Tokai-mura, Ibaraki 319-1195, Japan

Hiromasa Tanaka and Hiroshi Kudo

Department of Chemistry, Graduate School of Science, Tohoku University, Sendai 980-8578, Japan

Received: October 12, 2000; In Final Form: January 3, 2001

The structure of a hyperlithiated molecule has been deduced from an experiment for the first time. An analysis of the photoionization efficiency curve measured by laser-ablation time-of-flight mass spectrometry has revealed that the hyperlithiated Li_3O molecule is a floppy molecule with a "flat-bottomed" potential energy surface. The measured efficiency curve has a gradual linear rise from the threshold of 3.59 ± 0.02 eV up to the second onset of 4.4 ± 0.1 eV. An ab initio calculation reveals that such a "flat-bottomed" potential is realized with four closely located wells corresponding to one D_{3h} and three C_{2v} minima. The vibrational wave function spreads all over these minima even at the ground-state level. Also, this is the first evidence for "electronomers".

Introduction

A new concept of chemical bonding has been unveiled since the discovery of the Li_3O[1,2] and CLi_6[3] molecules, named "hyperlithiated molecules".[4] These molecules with excess valence electrons violate the octet rule, at least formally, and can be regarded as hypervalent molecules. Although these hyperlithiated molecules were confirmed to be thermodynamically stable toward dissociation to the corresponding octet molecules (Li_2O and CLi_4) and lithium atoms by experiments with Knudsen effusion mass spectrometry, their molecular structures have been discussed based only on theoretical calculations[4−7] without experimental evidence. Highly symmetric structures, such as O_h for CLi_6[6] and D_{3h} for Li_3O,[7] were predicted from the results of ab initio molecular orbital theory calculations by Schleyer's group. According to their calculation, the excess electrons beyond the octet rule are accommodated in an orbital which is antibonding between the central atoms (C and O) and the surrounding lithium atoms but is bonding among all the lithium atoms to form a lithium cage or network. Hyperlithiated molecules are also interesting species as a model system for investigating metal−insulator transitions because of their variable molecular and electronic structures.[8,9]

Trilithium oxide Li_3O was the first hyperlithiated molecule found in the equilibrium vapor over Li_2O crystals in 1978.[1] The dissociation energy for the loss of lithium atom ($Li_3O \rightarrow Li_2O + Li$) was measured as 212 ± 42 kJ/mol, and its existence was supported by an ab initio calculation (192 kJ/mol).[10] The ionization energy (IE) of Li_3O was measured by Wu et al.[2] and Lievens et al.[9] The latter value (3.54 ± 0.3 eV) is quite close to the theoretical vertical and adiabatic IEs (3.45−3.603 eV) reported by Schleyer's group[10,11] and Simons' group.[12] The minimal energy structure was predicted to have C_{2v} symmetry in the first theoretical study using Hartree−Fock self-consistent-field calculation,[5] but later, more sophisticated levels of theory suggested a D_{3h} structure,[7,9−12] which is widely accepted at present. Figure 1 shows molecular structures of neutral and cationic Li_3O calculated by a second-order Møller−Plesset perturbation theory (MP2/6-311+G(d)) using Gaussian 94.[13] For the neutral, both D_{3h} and C_{2v} symmetric structures are local minima on the potential energy surface at this level of theory. Single-point energy calculations at a more sophisticated level (CCSD(T)/6-311+G(d)) for both structures indicate that the D_{3h} structure is slightly favorable in energy, but the energy difference between those structures is much smaller than the accuracy of the calculation. The true minimal energy structure is, therefore, still unpredictable. Nevertheless, the C_{2v} structure is preferable even at 100 K, if the entropy is taken into account. We will demonstrate in this article that the profile of the ionization efficiency curve (IEC) would provide clues to the molecular structure and that the Li_3O molecule would take both the C_{2v} and D_{3h} structures even in the vibrational ground state.

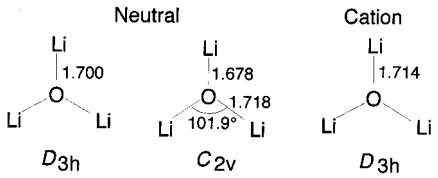

Figure 1. Calculated molecular structure of neutral and cationic Li_3O. There are two local minima (D_{3h} and C_{2v}) for the neutral. The D_{3h} structure is slightly favored in energy (0.8 kJ/mol) after the vibrational zero point energy correction. The calculations were carried out at the MP2/6-311+G(d) level of ab initio MO theory.

Experimental Section

We measured the IEC of Li_3O in a cluster beam generated by laser ablation. Details of the experiment are reported elsewhere.[14] Briefly, a lithium metal target was laser ablated by 532 nm pulses (8 mJ) from a frequency-doubled Nd:YAG laser (Continuum: SureliteII). The lithium vapor was reacted with water vapor which was synchronously injected into the clustering channel and entrained with pulsed helium carrier gas with a stagnation pressure of 0.9 MPa and then cooled through

* To whom correspondence should be addressed. E-mail: kei@beam.tokai.jaeri.go.jp.

10.1021/jp0037450 CCC: $20.00
Published on Web 04/04/2001

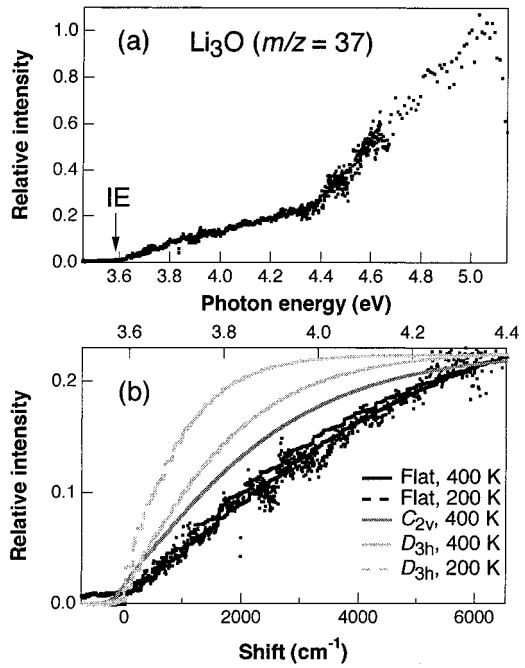

Figure 2. Photoionization efficiency curve measured for Li_3O (m/z = 37) generated by reactions of laser-ablated lithium metal with water vapor. The vibrational temperature of the supersonic beam was estimated as <200 K. (a) The curve shows a two-stage rise with the ionization threshold of 3.59 ± 0.02 eV and the second onset of 4.4 ± 0.1 eV. (b) Neither the D_{3h} nor C_{2v} structure gives a satisfying fit in the simulation. The good fit shown was obtained using an artificially flattened potential energy surface in the simulation.

supersonic expansion. After skimming at 14 cm downstream, jet-cooled lithium-containing species were photoionized in a time-of-flight mass spectrometer by frequency-doubled dye laser output (~1 mJ) (LambdaPhysik: SCANMATE2). Cations were accelerated to ~4 keV and detected by a microchannel plate after a 1 m field-free flight. Wavelengths of the ionizing laser beam were varied from 3.3 to 5.2 eV stepwise by 0.2 nm in width to measure the photon energy dependence of the signal intensity for m/z = 37 of Li_3O.

Experimental Results and Analysis

Figure 2a shows the IEC obtained for Li_3O. There are two prominent features in the profile of the IEC, that is, two-stage rise and gradual linear rise between the threshold and the second onset. The two-stage rise has already been reported by Lievens et al. [9] and attributed to some ionization processes other than the first ionization of Li_3O to give the ground state Li_3O^+ of current interest. Hence, we do not discuss the origin of the second rise further. We will focus on the first rise in this article. The threshold (3.59 ± 0.02 eV) determined with this curve is in excellent agreement with the theoretical ionization energy. Both the theoretical vertical and adiabatic ionization energies are calculated as 3.59 eV at the CCSD(T)/6-311+G(d) level of theory assuming the D_{3h} structure for the neutral geometry. This excellent agreement seems to support the reliability of the theoretical calculation on the minimal-energy structure. However, we are not necessarily fully satisfied at present.

The gradual linear rise between the threshold and the second onset seems remarkably long, and simulation and comparison of the IEC may provide some structural information. We can make simulations of the IEC for small molecules by a "direct counting of vibrational states" method, using the same procedure as described in our previous paper.[14] An essential idea of this simulation is to calculate Franck−Condon factors (FCF) within a harmonic approximation. The calculation includes the displacement of molecular geometry, the frequency change, and the normal mode rotation between the neutral and cationic states. All of these parameters can be computed by density functional theory (DFT) or ab initio MO theory calculations. As described in the previous paper,[14] the simulated IEC well reproduces the experimental curve for ionization processes of $Li_n(OH)_{n-1}$ clusters. Parameters calculated for the present simulation by the DFT (B3LYP/6-311+G(d)) method are listed in Table 1. In Figure 2b, the simulated IECs for Li_3O are superimposed on the experimentally observed IEC. The ionization of the D_{3h} structure of neutral Li_3O gives a step-function-like curve, which does not reproduce well the observed gradual linear rise even if any scale factors are applied to the amplitude. Even with parameters for the C_{2v} structure, the simulation is far from the observed linear rise of IEC. The well-fitted curve in Figure 2b was obtained when we artificially adjusted two in-plane bending frequencies to 10 cm^{-1} and restricted the neutral molecule to populate only on the zero-point level in these modes, that is, no vibrational excitation in these two bending modes.

We assumed a flat potential energy surface for the neutral Li_3O to reproduce the observed curve. Figure 3 shows the basic idea to explain why we examined with the flat potential. Figure 3a is the case for a small frequency change with a small displacement of minimal energy structures. Only the vibrational 0−0 band has a large FCF, and the integrated curve exhibits a step-function-like profile. This corresponds to the case of the D_{3h} structure of neutral Li_3O. Figure 3b is the case for a small frequency change with a large displacement of the minimal energy structure. Transition probabilities distribute over a broad range of energy shift. The integrated curve has a concave-up rise after some offset in energy, giving a relatively sharp "linear" rise and level-off leading to a plateau. Figure 3c is the case for ionization accompanied by a small displacement and a large frequency change due to a flat potential for the neutral. In this case, the transition probability does not decrease significantly over a wide range of energy shift, reflecting a large amplitude of vibrational motion on the neutral surface. The integrated curve shows a wide rise as observed in the present experiment. Throughout all these cases, the accessible energy range designated by ΔE in Figure 3 provides a crude measure for the width of rising in the IEC. That is, the observed gradual linear rise implies the flatness of the potential well of the neutral.

Ab Initio Calculations and Discussion

The ab initio MP2 calculation gives a very flat potential well in the two Li−O−Li bending modes: symmetric bending (scissoring) and asymmetric bending (rocking). Figure 4a shows a two-dimensional potential energy surface in the two bending coordinates: the horizontal axis for the scissoring and the vertical for the rocking. The other internal degrees of freedom are relaxed to give minimal energies at a given pair of bending angles. We can see a 3-fold flat bottom consisting of one D_{3h} minimum and three C_{2v} minima in Figure 4a. A cross-sectional view on the horizontal axis (φ = 0) shows a double well potential consisting of one of the three C_{2v} minima and the D_{3h} minimum (Figure 4b). The barrier height between the D_{3h} and C_{2v} minima is negligibly small (0.3 kJ/mol from the D_{3h} well). Consequently, the vibrational zero-point (v = 0) level, which is indicated by the horizontal solid line, lies above the barrier and thus spreads over these two minima. The v = 0 level was calculated by solving the Schrödinger equation directly with the one-dimensional potential energy surface. This wide v = 0

TABLE 1: Input Parameters for the Calculation of the Franck−Condon Factors

	frequencies (cm^{-1})			displacements ($cm^{1/1}$)		
		ν_l		k		
no.	ν_s	D_{3h}	C_{2v}	D_{3h}	C_{2v}	mode
1	249	81	103	0	0	out-of-plane bending
2	267	128	116	0	1451	symmetric in-plane bending
3	267	128	155	0	0	asymmetric in-plane bending
4	654	665	663	111	185	symmetric stretching
5	804	812	732	0	−81	asymmetric stretching
6	804	812	854	0	0	asymmetric stretching

Rotation Matrices, W^a

D_{3h}						C_{2v}					
1.00	0.00	0.00	0.00	0.00	0.00	1.00	0.00	0.00	0.00	0.00	0.00
0.00	1.00	−0.00	0.00	0.06	0.00	0.00	−1.00	0.00	−0.09	0.02	−0.00
0.00	−0.00	−1.00	0.00	0.00	0.06	0.00	−0.00	−0.99	−0.00	0.00	0.13
0.00	−0.00	0.00	1.00	0.00	0.00	0.00	−0.10	0.00	0.99	−0.09	−0.00
0.00	−0.06	0.00	−0.00	1.00	0.01	0.00	0.01	0.00	0.09	1.00	0.01
0.00	0.00	0.06	−0.00	−0.01	1.00	0.00	0.00	0.14	−0.00	−0.01	0.99

[a] Matrix elements W_{ij} present the mixing intensity between the ith mode of the cation and the jth mode of the neutral.

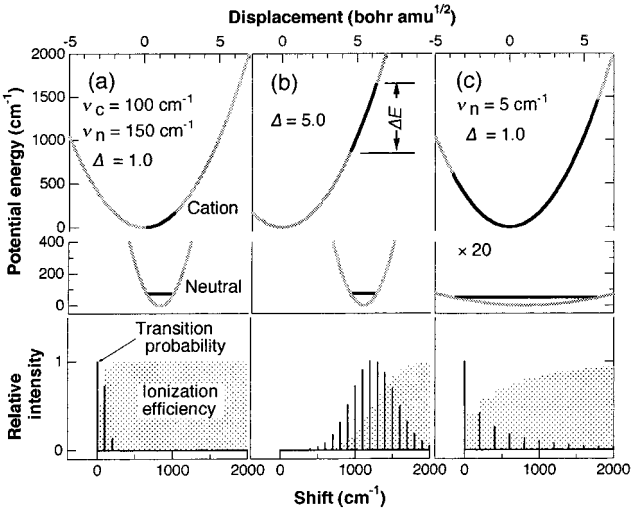

Figure 3. Relation between ionization efficiency curve (IEC) and potential energy curves in three cases of one-dimensional models. (a) A small displacement of energy minimum and small difference in frequency between neutral and cation result in a narrow Franck−Condon factor distribution and sharp rise of IEC. (b) A large displacement gives a concave-up rise of IEC. (c) A large difference in frequency with flat neutral potential gives a gradual rise. ν_c and ν_n indicate the vibrational frequencies of the cationic and neutral states, respectively.

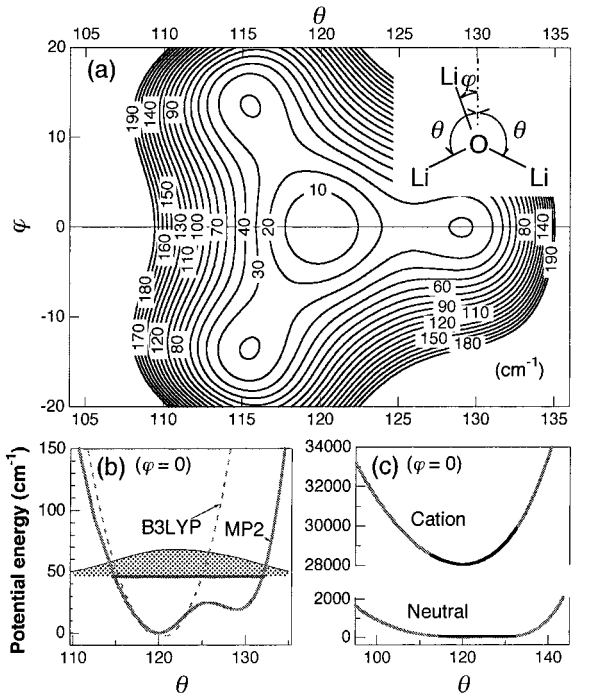

Figure 4. Ab initio potential energy surfaces of Li_3O. (a) The potential well consists of three C_{2v} minima and one D_{3h} minimum in the two bending motions. (b) The vibrational ground-state wave function spreads over the saddle points between the D_{3h} and C_{2v} minima. (c) The vertical ionization from the "flat-bottomed" potential accesses a wide energy range of the cation.

level indicates that the wave function of the vibrational ground state is delocalized over the three C_{2v} minima and the D_{3h} minimum. With this large amplitude of vibrational motion, a wide range of cationic potential energy surface is accessible by the vertical ionization from the $v = 0$ level as shown in Figure 4c. The accessible energy range ΔE (defined in Figure 3) is around 2000 cm^{-1}, and its order of magnitude is comparable with the observed width of linear rise (~6000 cm^{-1}).

We further discuss the validity of the simulation performed with the flat-bottomed potential. We cannot deal with the flat-bottomed potential directly in the Franck−Condon factor calculations due to the anharmonicity. Instead, we used only the $v = 0$ state of an extremely flat harmonic potential with a frequency of 10 cm^{-1} to obtain the fruitful fitting shown in Figure 2b. The amplitude of the $v = 0$ wave function on this potential is 3.47 in atomic units from the center of the well, i.e., the D_{3h} minimum. We should compare this artificial vibrational amplitude with that predicted from the two-dimensional ab initio potential to check the validity of the simulation. According to the normal coordinate for the symmetric bending, the artificial amplitude (3.47 au) corresponds to $\theta = 19.5°$. In Figure 4b, the far-side turning point of the $v = 0$ level is located at 12° away from the D_{3h} minimum. This means that the artificial amplitude is 1.6 times larger than the amplitude of the bending motion at 0 K predicted from the ab initio potential. This discrepancy is reasonable because of the following reasons.

(1) The real molecules populate on higher vibrational levels than $v = 0$. Assume that the vibrational temperature is 400 K, and the average vibrational energy becomes 280 cm^{-1}. This value indicates the turning point located at $\theta = 16°$, closer to the artificial value (19.5°).

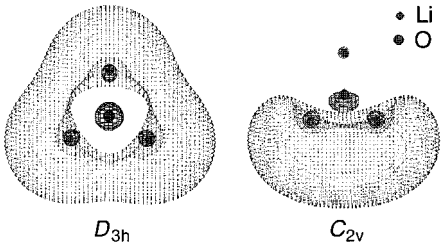

Figure 5. Typical isosurfaces of the singly occupied molecular orbitals of Li_3O. The excess electron is fully delocalized and forms a lithium cage in the D_{3h} structure, while it is localized and forms a salt consisting of Li_2^+ and LiO^- in the C_{2v} structure.

(2) The normal coordinate used in this comparison is not correct after a large geometric change. To evaluate the large amplitude correctly, distortion of the normal coordinate must be included. In the present case, Li−O stretchings are coupled with the bending. Therefore, the value of θ in Figure 4b does not represent the amplitude of a real vibrational wave function. The amplitude expressed by θ is just the projection to the normal coordinate and is always smaller than the real amplitude.

(3) With a given amplitude, real wave functions must show slower decay in the vibrational progression of FCFs than that given by the present simulation using the $v = 0$ harmonic functions. Because several vibrationally excited states ($v > 0$) contribute to the ionization, the wave functions distribute away from the center of the well in comparison with that of the $v = 0$ state. This fact indicates that an amplitude smaller than 3.47 au could reproduce the observed wide linear rise.

Therefore, the use of the $v = 0$ state of the artificially flattened harmonic potential is consistent with the ab initio flat-bottomed potential.

The most significant difference between the C_{2v} and D_{3h} structures is the shape of their singly occupied molecular orbitals (SOMO). The shape of the SOMO is an important characteristic for hyperlithiated molecules.[4−7] The D_{3h} structure shows fully delocalized SOMO (Figure 5), forming a lithium cage comprising all the three lithium atoms, similar to other hyperlithiated molecules. In contrast, the C_{2v} structure has SOMO localized on two lithium atoms to form one Li−Li bond and the remaining lithium atom is completely cationic with an natural atomic charge [15] of +0.95. Therefore, the C_{2v} structure can be regarded as a salt of Li_2^+ and LiO^-. In other words, the C_{2v} structure has an electronic structure segregated into metallic-like Li_2^+ and a lithium cation. Both the D_{3h} and C_{2v} structures have nearly the same stability. Theoretically, the existence of such nearly degenerate isomers with differing localization of their SOMOs in almost identical structures was predicted by Dorigo and Schleyer for hyperlithiated Li_2CN.[16] They called the isomers "electronomers". From this point of view, the C_{2v} and D_{3h} structures of Li_3O are electronomers, the evidence for which has been provided for the first time in the present experiment.

Surprisingly, the DFT-based calculation (B3LYP) gives a different potential shape. The potential well consists of only the D_{3h} minimum as seen in the broken curve in Figure 4b. With this potential curve, we can never reproduce the wide linear rise observed in the IEC. Therefore, the B3LYP surface is thought to be less realistic. The DFT calculation probably overestimates the stability of electron-delocalized structures, i.e., the D_{3h} structure in this case.

Conclusions

In summary, the IEC of the hyperlithiated Li_3O molecule was measured by photoionization-TOF mass spectrometry. From the simulations based on the FCFs, the observed gradual linear rise is ascribed to an extremely large amplitude of vibrational motion of the neutral Li_3O molecule. Ab initio MO calculations elucidated a flat-bottomed potential of Li_3O supporting the large amplitude of bending motion. The Li_3O molecule is a floppy molecule sharing both the hyperlithiated D_{3h} and segregated C_{2v} structures, which have nearly the same stability but are different in the localization of the SOMO. The present study provided the first evidence for this kind of molecular state called "electronomers", the presence of which had been theoretically predicted by Dorigo and Schleyer.[16]

References and Notes

(1) Kudo, H.; Wu, C. H.; Ihle, H. R. *J. Nucl. Mater.* **1978**, *78*, 380.
(2) Wu, C. H.; Kudo, H.; Ihle, H. R. *J. Chem. Phys.* **1979**, *70*, 1815.
(3) Kudo, H. *Nature* **1992**, *355*, 432.
(4) Schleyer, P. v. R. In *New Horizons of Quantum Chemistry*; Löwdin, P.-O., Pullman, B., Eds.; Reidel: Dordrecht, 1983; p 95.
(5) Schleyer, P. v. R.; Wurthwein, E.-U.; Pople, J. A. *J. Am. Chem. Soc.* **1982**, *104*, 5839.
(6) Schleyer, P. v. R.; Wurthwein, E.-U.; Kaufmann, E.; Clark, T. *J. Am. Chem. Soc.* **1983**, *105*, 5930.
(7) Wurthwein, E.-U.; Schleyer, P. v. R.; Pople, J. A. *J. Am. Chem. Soc.* **1984**, *106*, 6973.
(8) Tanaka, H.; Yokoyama, K.; Kudo, H. *J. Chem. Phys.* **2000**, *113*, 1821.
(9) Lievens, P.; Thoen, P.; Bouckaert, S.; Bouwen, W.; Vanhoutte, F.; Weidele, H.; Silverans, R. E.; Navarro-Vázquez, A.; Schleyer, P. v. R. *J. Chem. Phys.* **1999**, *110*, 10316.
(10) Rehm, E.; Boldyrev, A. I.; Schleyer, P. v. R. *Inorg. Chem.* **1992**, *31*, 4834.
(11) Zakrzewski, V. G.; Niessen, W. v.; Boldyrev, A. I.; Schleyer, P. v. R. *Chem. Phys. Lett.* **1992**, *197*, 195.
(12) Gutowski, M.; Simons, J. *J. Phys. Chem.* **1994**, *98*, 8326.
(13) Frisch, M. J.; Trucks, G. W.; Schlegel, H. B.; Scuseria, G. E.; Robb, M. A.; Cheeseman, J. R.; Zakrzewski, V. G.; Montgomery, J. A., Jr.; Stratmann, R. E.; Burant, J. C.; Dapprich, S.; Millam, J. M.; Daniels, A. D.; Kudin, K. N.; Strain, M. C.; Farkas, O.; Tomasi, J.; Barone, V.; Cossi, M.; Cammi, R.; Mennucci, B.; Pomelli, C.; Adamo, C.; Clifford, S.; Ochterski, J.; Petersson, G. A.; Ayala, P. Y.; Cui, Q.; Morokuma, K.; Malick, D. K.; Rabuck, A. D.; Raghavachari, K.; Foresman, J. B.; Cioslowski, J.; Ortiz, J. V.; Baboul, A. G.; Stefanov, B. B.; Liu, G.; Liashenko, A.; Piskorz, P.; Komaromi, I.; Gomperts, R.; Martin, R. L.; Fox, D. J.; Keith, T.; Al-Laham, M. A.; Peng, C. Y.; Nanayakkara, A.; Gonzalez, C.; Challacombe, M.; Gill, P. M. W.; Johnson, B.; Chen, W.; Wong, M. W.; Andres, J. L.; Gonzalez, C.; Head-Gordon, M.; Replogle, E. S.; Pople, J. A. *Gaussian 98*, Revision A.7; Gaussian, Inc.: Pittsburgh, PA, 1998.
(14) Tanaka, H.; Yokoyama, K.; Kudo, H. *J. Chem. Phys.* **2001**, *114*, 152.
(15) Reed, A. E.; Weinhold, F. *J. Am. Chem. Soc.* **1985**, *107*, 1919.
(16) Dorigo, A. E.; Schleyer, P. v. R. *Chem. Phys. Lett.* **1991**, *186*, 363.